# On the performance analysis of micro-hole drilling using magnetic field-assisted electrochemical spark machining

**Roopa Singh*, D. K. Singh, Jeeoot Singh**

*Madan Mohan Malaviya University of Technology, Gorakhpur, Uttar Pradesh, India*

Presented in International Conference on Precision, Micro, Meso and Nano Engineering (COPEN - 12: 2022)
December 8 - 10, 2022 IIT Kanpur, India

KEYWORDS

ECSM,
Magnetic Field,
Magnetohydrodynamic Effect,
Micro-Hole,
Overcut.

ABSTRACT

*Magnetic field-assisted electrochemical spark machining (MF-ECSM) is an advanced triplex hybrid machining technique which is precisely feasible for non-conductive and brittle materials such as glass. The advantage of MF-ECSM is that presence of magnetic field assists in improving the performance of machining due to the effect of magnetohydrodynamic convection (MHD). This paper presents a parametric study to observe the effect of voltage, NaOH concentration, tool rotational speed and magnetic field intensity on overcut during drilling of micro-holes on sodalime glass by in-house designed and fabricated MF-ECSM setup. The regression model based on experimental result has been used to correlate the input parameters and response. Analysis of variance showed the significance of individual parameters as well as their squares and interaction. This model has been further analysed using MATLAB to predict the effect of individual factors as well as their interaction on overcut by displaying surface and contour plots.*

## 1. Introduction

Non-conductive materials are widely used in microelectromechanical systems (MEMS), including lab-on-chip products and microfluidics devices. Due to its distinctive qualities, such as optical transparency, high rigidity, and exceptional chemical resistance, glass is used in a wide variety of applications. Glass, however, is brittle and typically difficult to machine using traditional methods. Nonconducting materials can be treated using the non-traditional machining technique known as electrochemical discharge machining (ECSM) (Xu & Jiang, 2021).

One of the complications in the ECSM process is clearing the debris from the machining gap. Accumulation of debris in the gap hinders the tool from reaching greater depths due to improper circulation of electrolyte in tool-workpiece gap. To overcome this problem, researchers have hybridized ECSM with magnetic field to enhance gas layer formation and circulation of electrolyte. Most of the researchers have used permanent magnet to study the effect of magnetic field on performance characteristics of ECSM. Cheng et al. (2010) used Nd-Fe-B ring magnet and drilled micro-holes in less than 20 s up to a depth of 450 µm. Hajian et al. (2021) observed that direction of bubble movement in electrolyte was driven by the orientation of magnetic field. Xu et al. (2018) presented an analytical explanation of MHD effect in enhancing the electrolyte circulation and machining performance. Rattan and Mulik (2017) used Nd-Fe-B ring magnet in traveling wire-ECSM and improved material removal rate by 200%. In the present work, an electromagnetic unit has been used to create magnetic field around the machining zone which created different magnetic field intensities and helped in removal of accumulated debris from the machining zone.

## 2. Experimental Setup

The experiments were carried out on an in-house developed setup of magnetic field-assisted electrochemical spark drilling (MF-ECSD). The setup consisted of an electrolyte tank which was filled with mixture of sodium hydroxide pellets and deionized water. Tungsten carbide drill bit with a diameter of 500 µm was chosen as the tool (cathode) and a graphite plate was made the counter electrode (anode). Sodalime glass slide (Thickness: 1 mm) was selected as the workpiece which was mounted between two threaded

*Corresponding author E-mail: singh.roopa91@gmail.com

https://doi.org/10.58368/MTT.22.5.2023.7-12

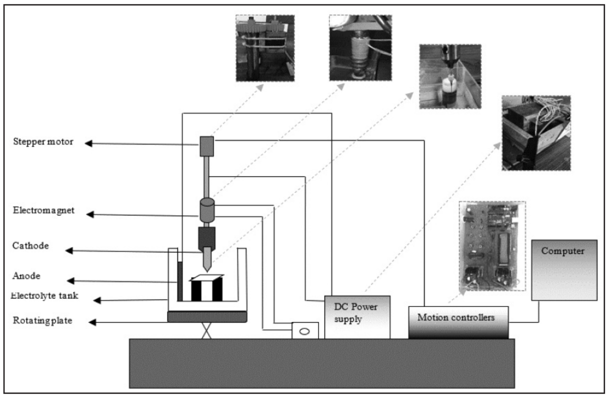


**Fig. 1.** Schematic diagram of MF-ECSD setup (Singh et al., 2022a; Singh et al., 2022b).

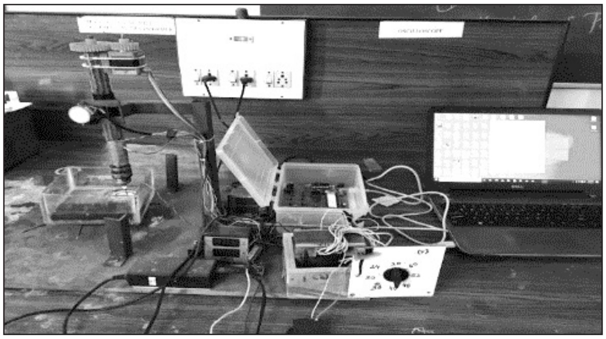

**Fig. 2.** Actual MF-ECSD setup.

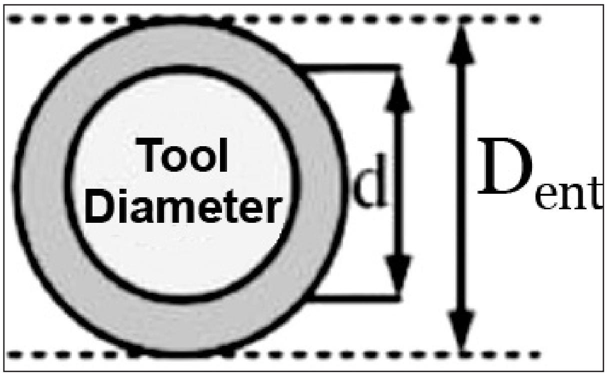


**Fig. 3.** Schematic diagram for computing overcut (Rajput et al., 2020).

fixtures made up of nylon. The cathode, anode and workpiece were submerged in the electrolyte for the machining to take place. Magnetic field was created around the machining zone with the help of an electromagnet made up of copper wire coiled around a spool and placed above the tool on the spindle. The spindle moved up and down and rotated with the help of a 12 V stepper motor. Voltage was applied between cathode and anode with the help of a power supply which was fabricated separately.

In the present study, voltage (V), NaOH concentration (NaOH conc.), tool rotational speed (TRS) and magnetic field intensity (MFI) were

**Table 1**
Input parameters and their level.

| Input parameters | Symbol | Unit | Coded levels | | |
|---|---|---|---|---|---|
| | | | -1 | 0 | 1 |
| V | $X_1$ | volts | 30 | 40 | 50 |
| NaOH conc. | $X_2$ | wt % | 25 | 30 | 35 |
| TRS | $X_3$ | rpm | 80 | 90 | 100 |
| MFI | $X_4$ | tesla | 0.00 | 0.09 | 0.18 |

**Table 2**
ANOVA of overcut.

| Source | Contribution | F-value | p-value |
|---|---|---|---|
| Model | 99.76% | 349.67 | 0.000 |
| Linear | 97.46% | 1195.72 | 0.000 |
| Square | 1.19% | 14.66 | 0.000 |
| Interaction | 1.10% | 8.97 | 0.001 |
| Lack-of-Fit | 0.24% | 13.49 | 0.071 |
| S=0.0004, $R^2$=99.76%, Adj. $R^2$=99.47% | | | |

selected as the input parameters and their range was set on the basis of trial experiments which is shown in Table 1. The experiments were planned and performed according to Box-Behnken layout of response surface methodology. For 4-factor 3-level, design, 27 experimental runs were performed. Overcut was chosen as the response to evaluate the performance of MF-ECSD. Overcut is the difference between entrance diameter of hole and diameter of tool electrode as shown in Fig 3.

A 2nd order regression model was obtained based upon experimental results which established the relationship between selected inputs (V, NaOH conc., TRS, MFI) and response (OC) and it is expressed as follows:

$$\begin{aligned}
\mathrm{OC\ (mm)} &= 0.699 + 0.00125X_1 - 0.02354X_2 - 0.00893X_3 \\
&-0.615X_4 + 0.000001X_1^2 + 0.000478X_2^2 + 0.000040X_3^2 \\
&+0.855X_4^2 - 0.000066X_1X_2 + 0.000081X_1X_3 + 0.01175X_1X_4 \\
&-0.000030X_2X_3 + 0.01167X_2X_4 - 0.00111X_3X_4
\end{aligned}$$

Table 2 shows the analysis of variance (ANOVA) of overcut. Lower p-values and higher F-value shows the significance of parameters and their interaction on overcut. The above equation has been further analysed using MATLAB to predict the effect of parameters beyond the selected range.

## 3. Results and Discussion

### *3.1. Effect of voltage on overcut*

Overcut rises with voltage which is evident from Fig. 4. Due to the electrolyte's joule heating caused by the constriction effect, more gas bubbles are produced at the tool's sidewall when a high applied voltage is used. Heat first reaches the top of the workpiece before descending to the bottom layers of the material. The thermal conductivity consequently increases at the top more quickly than it does at the bottom. As a result, the top surface has a bigger overcut. Jain et al. (1999) achieved a similar outcome.

### *3.2. Effect of NaOH concentration on overcut*

Fig. 5 shows that at moderate NaOH conc. values, overcut is minimised, but it increases as NaOH conc. rises. Antil et al. (2019) observed a comparable trend while performing an ECDM on composites made of a hybrid polymer. High current density brought on by high voltage and NaOH conductivity is the main cause of overcut.

### *3.3. Effect of tool rotational speed on overcut*

It is evident from Fig. 6 that the OC lowers as the tool's rotating speed rises. When moving at a higher speed, the sparking frequency is higher, which likely offers the work piece very little time to go through phase transition and reduces the overcut.

### *3.4. Effect of magnetic field on overcut*

According to Fig. 7, OC increases along with an increase in MFI. The better machining gap purification results in more active sparks when a magnetic field is introduced. The workpiece is forced to lose more material as a result of

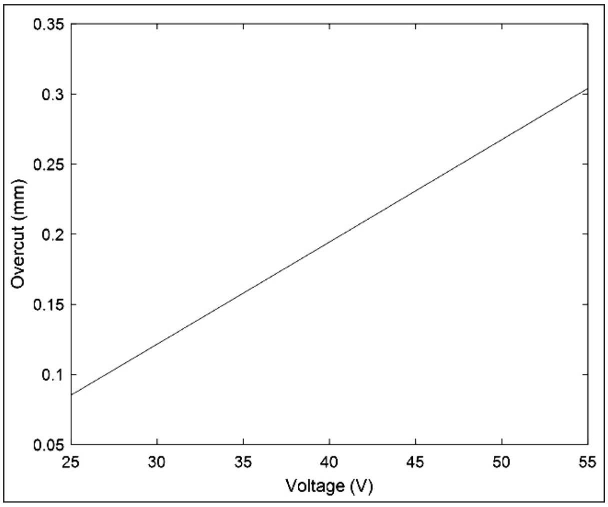


**Fig. 4.** Effect of voltage on overcut.

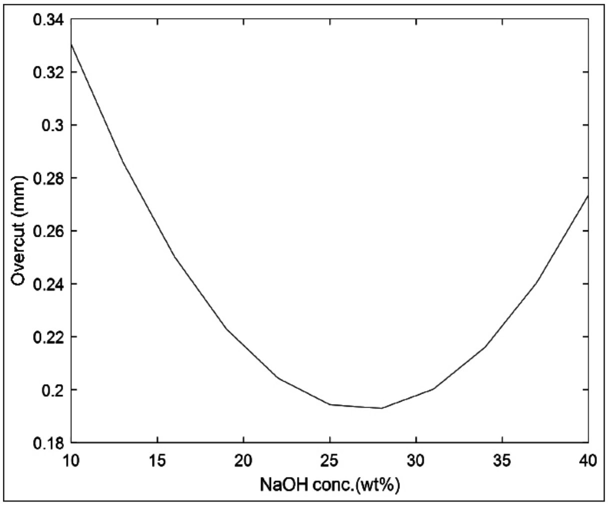


**Fig. 5.** Effect of NaOH conc. on overcut.

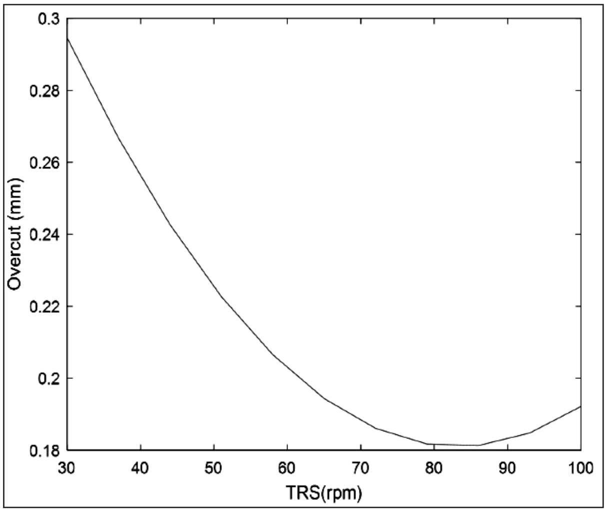


**Fig. 6.** Effect of tool rotational speed on overcut.

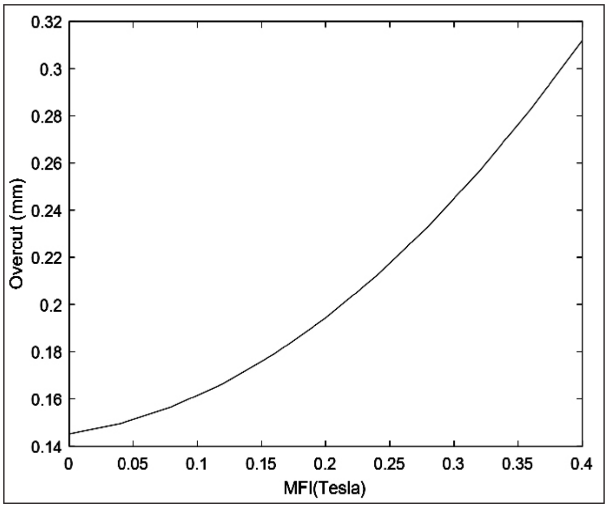


**Fig. 7.** Effect of magnetic field on overcut.

the sparking, and both the crater and oversize enlarge. Moreover, the magnetic force attracts machining waste, which it then drags out of the cutting gap. By being lodged between the sides of the cathode and workpiece, the debris melts due to discharges between the two thus expanding OC. Teimouri et al. (2012) produced comparable findings.

### *3.5. Effect of interaction of parameters on overcut*

The surface and contour plots based on regression models were analysed and generated using MATLAB. The hold values for analytical results were voltage - 40 V, NaOH conc. – 25 wt%, TRS – 90 rpm and MFI – 0.2 Tesla.

The interaction plot for V and NaOH conc. on overcut while maintaining constant TRS and MFI is shown in Fig. 8. The OC on the top surface grows in proportion to an increase in voltage. Heat first reaches the top of the workpiece before descending to the bottom layers of the material. The thermal conductivity consequently increases at the top more quickly than it does at the bottom. As a result, the top surface has a bigger overcut. Jain et al. (1999) achieved a similar outcome. At mild NaOH concentrations, overcut is minimised, but it increases as NaOH concentration rises. Antil et al. (2019) observed a comparable trend while performing an ECDM on composites made of a hybrid polymer. High current density, which is brought on by high voltage and NaOH conc. is the main cause of overcut. Around 27 V and 20 wt% was the minimum overcut (0.0823 mm) that could be achieved.

Fig. 9 shows the combined effect of V and TRS on overcut at constant NaOH conc. of 25 wt% and MFI of 0.2 Tesla. The interaction predicts that overcut increases with voltage and highest overcut is registered at 55 V. This is because the top surface of workpiece receives more heat from sparks than the bottom surface due to which more material removes from the entrance diameter. However, overcut reduces at moderate TRS due to less interaction time of workpiece surface. Sparking is not consistent on the surface of workpiece at higher speeds which results in reduced overcut.

Fig. 10 displays the collaborative effect of V and MFI when NaOH concentration and TRS are constant. With rise in voltage and magnetic field, overcut rises. Overcut occurs when the voltage increases because the top surface receives more heat from the sparks, which causes the hole to expand. With an increase in MFI, which has already been discussed, OC also rises.

Fig. 11 shows the interaction of NaOH conc. and TRS at constant V and MFI. Overcut reduces at

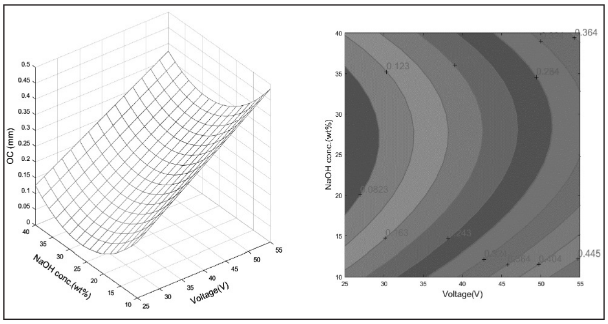


**Fig. 8.** Effect of voltage-NaOH conc. on overcut (TRS- 90 rpm, MFI-0.2 T).

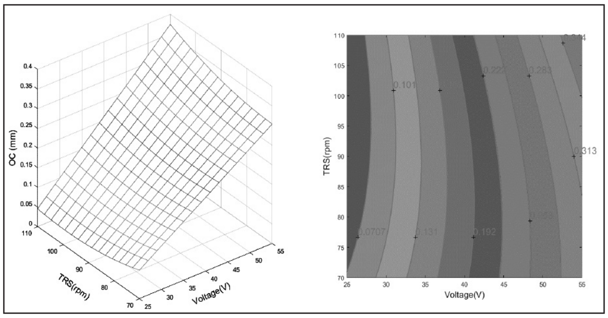


**Fig. 9.** Effect of voltage-TRS on overcut (NaOH conc.-25 wt%, MFI-0.2 T).

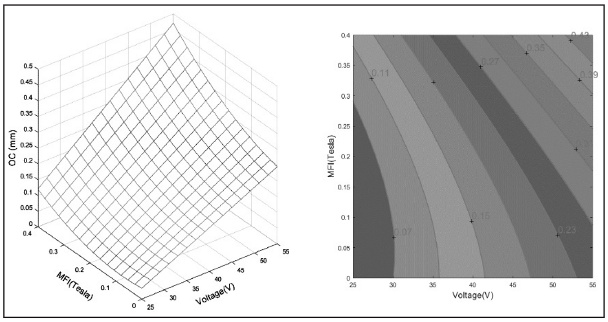


**Fig. 10.** Effect of voltage-MFI on overcut (NaOH conc.-25 wt%, TRS-90 rpm).

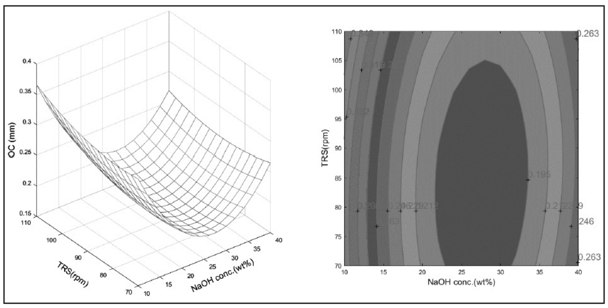


**Fig. 11.** Effect of NaOH conc.-TRS on overcut (voltage-40 V, MFI-0.2 T).

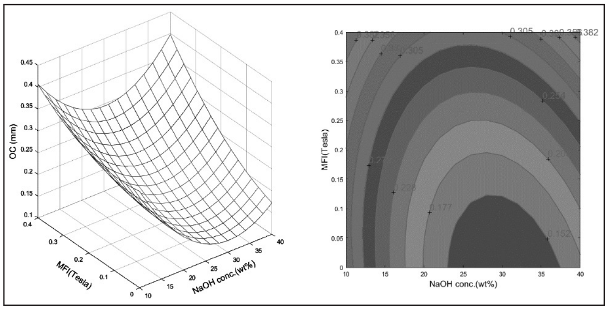

**Fig. 12.** Effect of NaOH conc.-MFI on overcut (voltage-40 V, TRS-90 rpm).

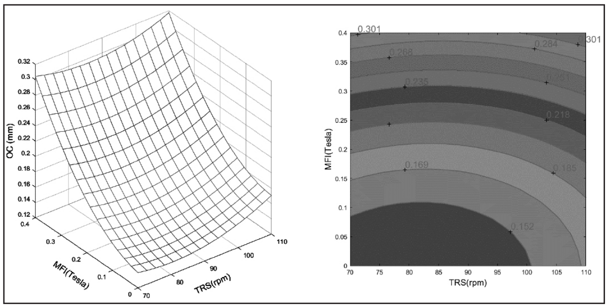

**Fig. 13.** Effect of TRS-MFI on overcut (voltage- 40 V, NaOH conc.- 25 wt%).

moderate NaOH concentrations and increases at higher concentrations. At higher concentrations, current density is high which causes increase in overcut. Similarly, at moderate TRS, overcut reduces and increases thereafter.

Fig. 12 shows the interaction of NaOH conc. and MFI when V and TRS are constant. At moderate values of NaOH conc., overcut was less and it increased at higher levels of concentration. Current density is high at higher concentrations which expands overcut. An increase in MFI improves overcut because drilling zone particles adhere to the cathode walls and melt during sparking, expanding the drilled hole. At 0 T and 23 wt% NaOH conc., lowest overcut (0.152 mm) was reached. In an experiment, a parametric setup of 30 V, 30 wt%, 90 rpm, and 0 T resulted in the lowest possible OC.

Fig. 13 shows the interaction of TRS and MFI at constant V and NaOH conc. Rise in TRS increases centrifugal force and magnetic field generates Lorenz force. The combined effect of centrifugal force and Lorenz force assists in exclusion of additional debris from the machining zone. Fragments of the removed debris adheres to the sides of tool and melts during sparking which increases overcut. Lowest overcut (0.152 mm) was attained in the absence of magnetic field and at 100 rpm.

## 4. Conclusions

In this study, experiments have been performed on an in-house developed MF-ECSM setup where an electromagnet was used to generate magnetic field of different intensities. Parametric analysis shows the effect of different parameters namely voltage, NaOH concentration, tool rotational speed and magnetic field intensity on overcut. The prediction of effect of individual parameters and their interaction beyond the selected range by analysing the regression equations using MATLAB shows that

1. Overcut increased with increase in voltage.
2. Overcut decreased then increased with increase in NaOH concentration. Optimum overcut was obtained at around 25 wt% NaOH concentration.
3. Overcut decreased with increase in tool rotational speed. Optimum overcut was obtained at around 80 rpm.
4. Overcut reduces at moderate values of NaOH and higher tool rotational speeds but expands with voltage and magnetic field intensity.
5. Highest overcut was registered at 55 V and 0.4 Tesla. Low overcut was obtained at around 23 wt% NaOH concentration and at 100 rpm.

## References


Antil, P., Singh, S., & Manna, A. (2019). Experimental Investigation During Electrochemical Discharge Machining (ECDM) of Hybrid Polymer Matrix Composites. *Iranian Journal of Science and Technology - Transactions of Mechanical Engineering*, https://doi.org/10.1007/s40997-019-00280-5.

Cheng, C. P., Wu, K. L., Mai, C., & Hsu, Y. S. (2010). Magnetic field-assisted electrochemical discharge machining. *Journal of Micromechanics and Microengineering*, *20,* 75019-75017.

Hajian, M., Razfar, M. R., & Movahed, S. (2021). An experimental study on the effect of magnetic field orientations and electrolyte concentrations on ECDM milling performance of glass. *Precision Engineering*, *45,* 322-331.

Jain, V. K., Dixit, P. M., & Pandey, P. M. (1999). On the analysis of the electrochemical spark machining process. *International Journal of Machine Tools and Manufacture, 39,* 165-186.

Rajput, V., Pundir, S. S., Goud, M., & Suri, N. M. (2020). Multi-Response optimization of

ECDM parameters for silica (Quartz) using grey relational analysis. *Silicon*, https://doi.org/10.1007/s12633-020-00538-7.

Rattan, N., & Mulik, R. S. (2017). Improvement in material removal rate (MRR) using magnetic field in TW-ECSM process. *Materials and Manufacturing Processes*, *32,* 101-107.

Singh, R., Singh, D. K., & Singh, J. (2022). Experimental investigations and multi-response optimization of dynamic magnetic field-assisted electrochemical spark drilling using grey relational analysis. *Journal of Advanced Manufacturing Systems*, https://doi.org/10.1142/S0219686723500117, 2022.

Singh, R., Singh, D. K., & Singh, J. (2022). Modeling and optimisation of magnetic field assisted electrochemical spark drilling using hybrid technique. *Advances in Materials and Processing Technologies*, 10.1080/2374068X.2022.2118934.

Teimouri, R., & Baseri, H. (2012). Experimental study of rotary magnetic field-assisted dry EDM with ultrasonic vibration of workpiece. *International Journal of Advanced Manufacturing Technology*, *67,* 1371-1384.

Xu, Y., Chen, J. H., Jiang, B. Y., Liu, Y., & Ni, J. (2018). Experimental investigation of magnetohydrodynamic effect in electrochemical discharge machining. *International Journal of Mechanical Sciences*, *142-143*, 86-96.

Xu, Y., & Jiang, B., (2021). Machining performance enhancement of deep micro drilling using electrochemical discharge machining under magnetohydrodynamic effect. *International Journal of Advanced Manufacturing Technology*, *113*, 883-892.

**Roopa Singh** is currently pursuing her Ph.D from Department of Mechanical Engineering at Madan Mohan Malaviya University of Technology, Gorakhpur. She completed her Masters in Manufacturing Engineering and Management from Govind Ballabh Pant University of Agriculture and Technology, Pantnagar, Uttarakhand. Her area of interest is advanced manufacturing technology. She has published research papers in reputed international journals.

**Dr. D. K. Singh** is currently working as Professor in Mechanical Engineering Department at Madan Mohan Malaviya University of Technology, Gorakhpur. He obtained his Ph.D from Indian Institute of Technology, Kanpur in 2006. He has one patent on “A Method for Magnetic Abrasive Finishing using a Pulsating Flexible Magnetic Abrasive Brush and a Magnetic Abrasive Finishing Device”. He has published more than 45 research papers in reputed International/National journals and International/National conferences. He has also organized/attended various seminars / workshops / conferences in various fields. He has delivered invited talks in IITs/NITs/state engineering colleges. (E-mail: dksme@mmmut.ac.in)

**Dr. Jeeoot Singh** is currently working as Professor in Mechanical Engineering Department at Madan Mohan Malaviya University of Technology, Gorakhpur. His area of interest are Computational mechanics, Mechanical modelling of laminated, sandwich and FGM plate using radial basis function, Linear and nonlinear bending, buckling and vibration of FGM, laminated and sandwich plate, Saint-Venant torsion analysis and Radial basis function based meshfree method. He has 20 years of teaching and research experience in reputed institutes. He has published more than 70 papers in reputed national and international journals. (E-mail: jsme@mmmut.ac.in)